Polarized dark solitons in isotropic Kerr media

Adrian P. Sheppard
Service d'Optique et Acoustique, Université Libre de Bruxelles, Campus du Solbosch, Code Postale 194/5, B-1050 Bruxelles, Belgium

Yuri S. Kivshar
Australian Photonics Cooperative Research Centre, Research School of Physical Sciences and Engineering, Optical Sciences Centre, Australian National University, Canberra ACT 0200, Australia

(Received 29 October 1996)

We characterize dark-type vector optical solitons of arbitrary polarization in isotropic, Kerr-type media by applying Hirota's method to the integrable Manakov model with a defocusing nonlinearity. We find that nonuniformly polarized solitons comprise a rich solution family that can be divided into two categories: dark-dark and dark-bright vector solitons. We consider the propagation dynamics and the interactions of these vector solitons by deriving multisoliton solutions, and show the existence of stationary bound states, a phenomenon not observed for scalar dark solitons. [S1063-651X(97)10404-4]

PACS number(s): 42.65.Tg, 42.81.Dp, 03.40.Kf

I. INTRODUCTION

The theory of solitons and solitary waves has turned out to be relevant to a variety of different physical processes. However, it is in the field of guided wave optics that solitons have made the greatest experimental impact. Optical fiber transmission systems have been realized using temporally confined solitons propagating as pulses in one dimension [1]. More futuristically, nonlinear switches that rely on the interaction between spatially confined solitons are being investigated in a variety of media [2–4]. Solitons on a background field, also known as dark solitons, typically appear as localized intensity dips on a finite carrier wave [5], and, like their bright counterparts, have been observed in fibers [6] and waveguides [7]. They are generally more robust than bright solitons, and have been the object of recent research considering the influence of polarization [8–10].

In general, the nonlinear response of isotropic materials can be anisotropic, as can be seen from a phenomenological analysis of the symmetries of the higher-order susceptibility tensors $\chi^{(n)}$ [11]. However, in the simplest model of a nonlinear medium, one assumes that the medium is completely characterized by a refractive index change which depends only on the total intensity. This model is valid for electrostrictive media, and materials in which the nonlinearity is slightly nonlocal in either space or time [12]. Many liquids and gases fall into this category. It has also been shown, both numerically [13] and now analytically [14], that the anisotropy induced in silica fibers averages to zero over long propagation distances on account of stochastic variations in the fiber characteristics. More concretely, recent spatial soliton experiments [15,16] have shown that $Al_xGa_{1-x}As$ semiconductors, operated at the half-band-gap, can also be entirely isotropic at the nonlinear level.

Studying the propagation of quasimonochromatic, paraxial light beams, and considering only an isotropic third-order (Kerr) nonlinear response, one may derive the Manakov model for paraxial light beams in diffractive media [17], including semiconductors operated at the half-band-gap [19], and for wave packets in dispersive optical fibers [18,14]. The Manakov equation is a vector nonlinear Schrödinger (NLS) equation possessing the symmetry of the second unitary $[U(2)]$ group, and was shown by Manakov [17] to be integrable. He integrated it by extending the method of the inverse scattering transform (IST), that had already been used to integrate the Korteweg–de Vries equation and the scalar $[U(1)]$ NLS equation [20]. This enabled him to characterize the interaction between two bright solitons of arbitrary polarization. The spectral problem associated with the Manakov equation is 3×3, and analytical investigation tends to be frustrated by algebraic complexity which is exacerbated by the noncommutativity of the underlying $U(2)$ symmetry group. There was, until recently, little addition to the original work of Manakov.

While the scalar nonlinear Schrödinger equation was solved many years ago for nonzero boundary conditions [21], no such work has been completed for the Manakov equation. Perhaps researchers believed that the constraints imposed by the nonzero background field would reduce it to a simple generalization of the scalar NLS equation. In any case application of the IST to the Manakov equation with nonzero boundary conditions is no small task, involving the study of three-sheet Riemann surfaces. Recently [10], the Hirota method was applied to the Manakov equation as a more straightforward way of deriving explicit bright and dark N-soliton solutions. Unfortunately, owing to an oversight, the authors find solutions that are apparently only trivial generalizations of solutions to the scalar NLS equation.

This work examines particularly the dark solitons that one finds in systems described by the Manakov model with a defocusing nonlinearity. Considering the field to be composed of two orthogonally polarized field components, there are two possible ways to generalize a scalar dark soliton formed in one component only. The second field component may also form a kink structure, or it may be localized in the region of the dark soliton. These two classes turn out to be fundamentally different. This study will characterize these individual solitons, then use the Hirota method to search for the multisoliton solutions which describe elastic soliton in-

teractions in the absence of radiative components. The types of solutions one obtains from an analytical study of this sort are constrained by the infinity of conservation laws possessed by all the soliton equations. One can predict in advance the usual soliton properties: solitons survive all collisions with their amplitude and direction intact, but may suffer changes in their position and phase. In this paper we will highlight particularly the less evident effects of the interplay between the polarization components.

II. HIROTA'S METHOD AND DARK-TYPE MANAKOV SOLITONS

A. General formalism

The Manakov model for describing the $(1+1)$-dimensional stationary propagation of light of arbitrary polarization in defocussing media leads to the $U(2)$ nonlinear Schrödinger (NLS) equation [17,14,19]

$$i\frac{\partial \mathbf{e}}{\partial z}+\frac{1}{2}\frac{\partial^2 \mathbf{e}}{\partial x^2}-|\mathbf{e}|^2\mathbf{e}=\mathbf{0}, \tag{1}$$

where x and z are the transverse and longitudinal coordinates respectively, and $\mathbf{e}(x,z)$ is a two-component vector describing transversely polarized light. It is easiest to decompose $\mathbf{e}$ into orthogonal polarization components; we choose the labels $e_+(x,z)$ and $e_-(x,z)$ as the envelopes of two arbitrary but orthogonal polarizations, in which Eq. (1) reads

$$i\frac{\partial e_\pm}{\partial z}+\frac{1}{2}\frac{\partial^2 e_\pm}{\partial x^2}-(|e_+|^2+|e_-|^2)e_\pm=0 \tag{2}$$

If we confine the light to a single polarization state, say e_+, then the problem reduces to the $U(1)$ NLS equation that possesses as soliton solutions the family of dark solitons. The most general expression for the dark soliton is

$$e_+=\tau\{i\sin\phi+\cos\phi\,\tanh[a(x-bz)]\}e^{icx+i[c^2/2+\tau^2]z}. \tag{3}$$

The dark soliton induces a corresponding change of the medium refractive index change which is proportional to the total field intensity

$$\Delta n^2=|\mathbf{e}|^2=\tau^2-a^2\ \operatorname{sech}^2[a(x-bz)], \tag{4}$$

where $\phi=\arctan[(c-b)/a]$, and the soliton parameters are connected by the constraint $a^2+(c-b)^2=\tau^2$, otherwise written as $a=\pm\tau\cos\phi$. The soliton therefore exists in the domain $c-\tau<b<c+\tau$. It describes a localized kink structure on a background plane wave; τ gives the amplitude of the background, while c gives its direction. Across the soliton, there is a phase jump in the background wave of $\pi-2\phi$, topologically trapping the soliton. The contrast of the soliton, defined as the ratio between the maximum and minimum intensities, is given by $\cos^2\phi$. Note that after having defined the background field (by fixing τ and c), the soliton is characterized completely by the single parameter b; the width, contrast, and phase jump are all defined by it. For $b=c$, we have a black soliton of unity contrast, and a π phase shift traveling parallel to the background wave, while, as $b\to c\pm\tau$ (or $\phi\to\pi/2$), the soliton contrast and the phase shift both drop to zero.

When considering solitons of nonuniform polarization, and thereby introducing the field component e_-, one has the option to either localize e_- by restricting its intensity to zero for $x\to\pm\infty$, or leave it delocalized with any finite intensity at infinity. We shall see in the course of this paper that these two cases are fundamentally different. The unrestricted case leads to more traditional vector dark solitons of the type that were considered in [8] and [10], in which there is an intensity dip in both polarization components at the center of the soliton. We call these dark-dark solitons, since both components describe a dark-type mode. Localizing the field leads to dark-bright solitons, first investigated in [9], in which the e_- component is a bright localized mode confined by the presence of the other component.

To characterize these Manakov dark solitons, we apply the method of Hirota [22], and first transform Eq. (2) into a bilinear form. We do this by introducing the Hirota functions $f(x,z)$, $g(x,z)$, and $h(x,z)$, such that

$$e_+=g/f \quad \text{and} \quad e_-=h/f. \tag{5}$$

There is no loss of generality in assuming f to be real. Expressing the Manakov equations in terms of f, g, and h is simplified by making use of the Hirota bilinear operator

$$D_x^m D_z^n(f\cdot g)=(\partial_x-\partial_x')^m(\partial_z-\partial_z')^n \times[f(x,z)g(x',z')]|_{x=x',z=z'}. \tag{6}$$

The Manakov equation can now be written in the simple forms

$$B_1(g\cdot f)=0, \quad B_1(h\cdot f)=0, \tag{7}$$

$$B_2(f\cdot f)=-|g|^2-|h|^2, \tag{8}$$

where B_1 and B_2 are bilinear operators defined by

$$B_1=iD_z+\tfrac{1}{2}D_x^2-\chi, \quad B_2=\tfrac{1}{2}D_x^2-\chi.$$

Following [10], we introduce the parameter χ, necessary for the search for dark solitons. Considering plane-wave solutions of the form $e_\pm=e_\pm^o e^{i\mathbf{k}_\pm\cdot\mathbf{r}}$ leads to the identity $|e_+^o|^2+|e_-^o|^2=\chi$, which shows that χ, which must be real, dictates the total intensity of the background field.

Once an equation has been written in a bilinear form, Hirota's method proceeds by assuming that each Hirota function can be written as a polynomial function of an arbitrary parameter λ. The theoretical basis for this approach is still not well understood. Nevertheless, it is clear that the Hirota method provides a convenient prescription for finding closed-form analytical solutions to many, if not all, of the soliton equations.

B. Dark-dark solitons

Our initial task is to find individual, static, dark-dark solitons. To do this we introduce an ansatz normally used for finding topological solitons:

$$g=g_0(1+\lambda^2 g_2),$$

$$h=h_0(1+\lambda^2 h_2) \quad \text{and} \quad f=1+\lambda^2 f_2. \tag{9}$$

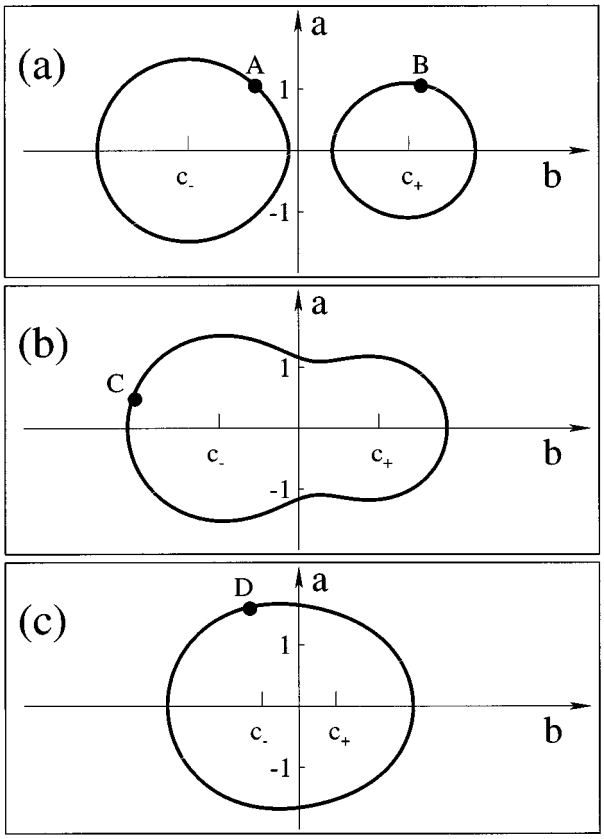

FIG. 1. The single dark-dark soliton in (b,a) space. The soliton exists on the curves defined by Eq. (13), presented here for three different background fields. The backgrounds in e_+ and e_- become more closely aligned in descending from (a) to (c). In (a), (b), and (c), $\tau_+=1.0$, $\tau_-=\sqrt{2}$, and $c_+=-c_-=c$. (a) $c=1.8$, (b) $c=1.3$, and (c) $c=0.6$. The points labeled *A*, *B*, etc. correspond to the solitons shown in Fig. 2.

We substitute Eqs. (9) into Eqs. (8), then equate powers of the arbitrary parameter λ. There will be three equations at each of the zeroth, second, and fourth powers in λ. If we can satisfy all these equations, then we will have found a closed-form solution to the problem. In practice, the last half of the equations are redundant—a correct solution will be defined completely by the identities up to the second power in λ. One may solve these equations by considering one order at a time, commencing at the zeroth order. Following this procedure results in a ''dark-dark'' vector soliton of the following form:

$$e_\pm=\tau_\pm\{i\ \sin\phi_\pm+\cos\phi_\pm\tanh[a(x-bz)]\}\times e^{ic_\pm x+i[c_\pm^2/2+\chi]z}, \tag{10}$$

with $\phi_\pm=\arctan[(c_\pm-b)/a]$. The soliton parameters are connected by the identity

$$a^2=\tau_+^2\cos^2\phi_++\tau_-^2\cos^2\phi_-\,. \tag{11}$$

This is an implicit identity, since ϕ_+ and ϕ_- each depend on a. The intensity is the same form as for the scalar soliton,

$$|\mathbf{e}|^2=\tau^2-a^2\mathrm{sech}^2[a(x-bz)] \tag{12}$$

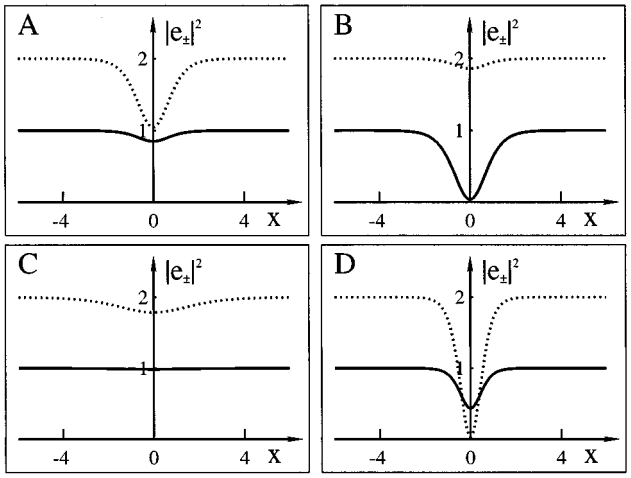

FIG. 2. Some examples of the intensity profiles of the single dark-dark soliton, taken from the previous figure. *A*: $b=-0.7$. *B*: $b=2.0$. *C*: $b=-2.7$. *D*: $b=-0.8$. It is clear that this is a rich and varied family of solutions.

The background field on which these solitons repose may be thought of as two superposed plane waves whose intensity and direction of travel can be independently chosen. Specifying the background field leaves us with only *one* degree of freedom for the soliton itself, as for the scalar dark soliton. We use the soliton direction b as the independent variable; the soliton width (defined by $1/a$), and the soliton ''greyness'' parameters ϕ_+ and ϕ_- are then uniquely defined through Eq. (11).

We illustrate the characteristics of this soliton with the aid of Figs. 1, 2, and 3. In Fig. 1 we show the soliton's domain of existence in (b,a) space, for several different examples of background fields. Remember that $1/a$ defines the soliton width, and $\arctan b$ is the propagation angle relative to the z axis. Therefore at the right of each plot we find the rightwards-moving solitons and, at the left, leftwards moving ones. Figure 1(a) illustrates a case of highly disparate background fields (i.e., in which c_+ is very different from c_-), and dark-dark solitons are found that approximately follow each field direction, i.e., roughly in the range $c_\pm-\tau_\pm\leqslant b\leqslant c_\pm+\tau_\pm$. Note that at the points $b=c_\pm$ the contrast in the field $e_\pm$ is unity—the soliton is ''black'' in that

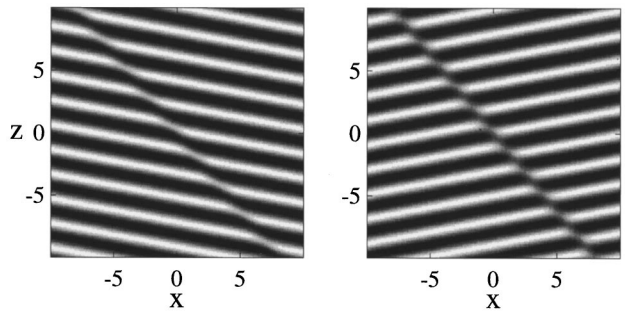

FIG. 3. The phase dependence of the two components of a single dark-dark soliton, here the case *D* from Figs. 1 and 2. The component e_+ is shown at left, e_- at right. The soliton is propagating up the page and is clearly shown to be a dark soliton propagating across two different superimposed background fields.

component (although the total contrast will be less than unity). For widely disparate backgrounds the existence criterion Eq. (11) reduces to $a \simeq \pm \tau_{\pm} \cos\phi_{\pm}$, i.e., the fields decouple from each other. A good example of this is shown in Fig. 2(C), where the soliton component in e_- is influenced only minimally by the other field e_+ whose profile is almost constant. In the opposite limit of closely aligned fields $c_+ \to c_- \to c$ the solitons describe scalar dark solitons whose parameters are connected through the identity $a^2+(b-c)^2 = \tau_+^2 + \tau_-^2$.

C. Dark-bright solitons

We now turn our attention to the dark-bright solitons in which the field component e_- is localized by the waveguide induced by e_+. To find individual, static, dark-bright solitons we introduce, for h, an ansatz typically regarded as suitable for bright solitons, and one for g appropriate for kinks:

$$g = g_0(1+\lambda^2 g_2), \quad h = \lambda h_1 \quad \text{and} \quad f = 1+\lambda^2 f_2. \tag{13}$$

On substituting this into the Hirota equations (8), and following the same procedure as above (see Sec. I of the Appendix), one derives the dark-bright soliton

$$e_+ = \tau\{i \sin\phi + \cos\phi \tanh[a(x-bz)]\} e^{icx + i[c^2/2+\tau^2]z}, \tag{14}$$

$$e_- = \sqrt{\tau^2\cos^2\phi - a^2}\ \mathrm{sech}[a(x-bz)] e^{ibx + i[(a^2-b^2)/2-\tau^2]z}, \tag{15}$$

where ϕ, as before, is defined by $\phi = \arctan[(c-b)/a]$, and the solution is valid only when the inequality $a^2 + (c-b)^2 \leqslant \tau^2$— or $a^2 \leqslant \tau^2\cos^2\phi$— is satisfied. When this constraint is satisfied as an equality, the intensity in e_- is zero, and the scalar dark soliton is recovered. The replacement of a strict equality by an inequality adds a degree of freedom to the system— a and b can now be chosen independently. This additional degree of freedom ordains the dark-bright soliton with some interesting properties. The dark component takes the dark soliton profile, but, as compared to the dark soliton, the contrast at a given propagation angle is reduced by the antiguiding bright component. Contrary to the dark-dark soliton, in this case the two fields work against one another to the point that the nonlinear change induced by e_+ can be canceled by the nonlinear change of e_-. The total intensity is again the same,

$$|\mathbf{e}|^2 = \tau^2 - a^2\ \ \mathrm{sech}^2[a(x-bz)]. \tag{16}$$

Figure 4 shows the existence domain of the dark-bright solitons, as defined by the constraint $a^2+(c-b)^2 \leqslant \tau^2$. On the perimeter of this domain are the scalar dark solitons. Note that the dark-dark solitons exist only outside this domain—in the region $a^2+(c-b)^2 \geqslant \tau^2$. This reflects the fact that the additional dark component adds to the refractive index change while the localized ''bright'' component reduces it. One can view the scalar dark soliton as the common ground between the dark-dark and the dark-bright solitons. On the center line $b=c$, the black-bright solitons are found, while

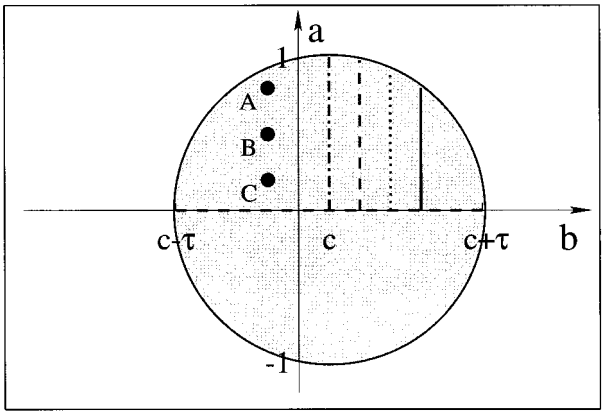

FIG. 4. The domain of existence of the dark-bright solitons for $c=0.2$ and $\tau=1$. The soliton is found anywhere within the circle—it is a two parameter family on a given background. On the perimeter the soliton becomes a scalar dark soliton without a bright component. The labeled points and the vertical lines correspond to the examples shown in Fig. 5.

near the b axis we find the low contrast, broad solitons for which the width goes to infinity ($a \to 0$) and the contrast to zero.

At the top left of Fig. 5 we show how the power in each field component varies, as we traverse the range of values of a for various fixed b. Notice that a scalar soliton of low contrast (i.e., very grey, traveling across the background wave) can only support a small amount of power in the bright component before its width goes to infinity and contrast to zero. At the other end of the scale, a black-bright soliton (i.e., $b=c$) can ultimately support an infinite power in the guided component when its width goes to infinity. The remainder of Fig. 5 shows the profiles of three different dark-bright solitons, labeled A, B, and C from Fig. 4. In these examples we witness the degeneration of a dark soliton: in-

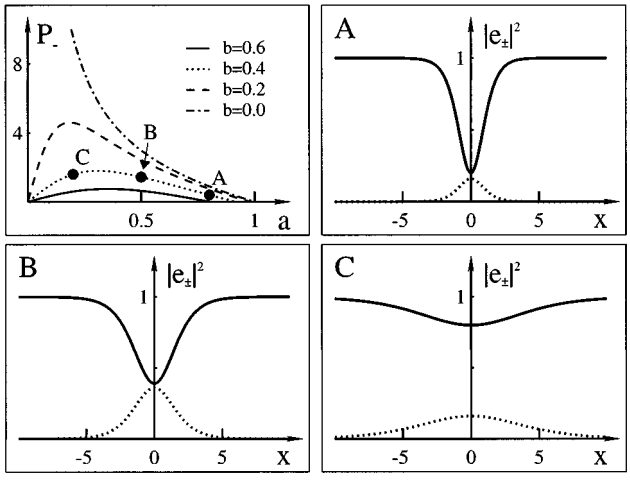

FIG. 5. At the top left we show the dependence of P_-, the power in the bright component e_-, on the soliton width a for several values of the direction b. The lines here correspond to those of the same style from Fig. 4. The rest of the figure shows examples of dark-bright soliton profiles, with parameters $b=-0.2$, and (A) $a=0.8$, (B) $a=0.5$, and (C) $a=0.2$. Note the antiguiding character of the bright component—its effect is to reduce the total guidance, thus ''greying out'' the soliton.

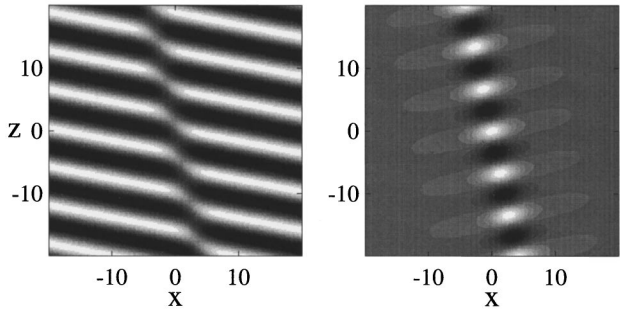

FIG. 6. The phase dependence of a dark-bright soliton. The dark component e_+ is at left, the bright component e_- at right. It is most apparent in this figure that the component e_- is following the waveguide induced for it by e_+.

creasing the parameter a reduces the contrast until the soliton disappears into the background. Figure 6 shows the phase variation of the propagating soliton of case A.

III. SOLITON INTERACTIONS

For integrable models one expects to find analytic solutions not merely for the solitons themselves, but for all the solutions that characterize their interaction in the absence of a nonsolitonic, radiative component. We perform this calculation only for dark-bright solitons. Finding multisoliton solutions is simply a question of taking a breath and extending the Hirota method to higher orders. Using straightforward but messy algebra, as described in Sec. 2 of the Appendix, one derives the two-soliton expression of Eq. (A17). The analytical formula is not very informative of itself, and we must resort to asymptotics and numerics to characterize and visualize it. Consider the regions of (x,z) space where the two solitons are well separated. One should note first that when the soliton directions coincide, we can form a bound state, in which the solitons never separate. We will return to this bound state later on. Let us take $b_1 > b_2$ so that soliton 1 crosses soliton 2 from left to right as z increases. In accordance with the ''nonlinear superposition principle,'' one expects no change after the crossing, except for a small displacement of the center of each soliton. Using simple asymptotics, we obtain these displacements from Eq. (A17),

$$\Delta x_1 = \frac{1}{a_1}\left(\left| \frac{\kappa_1 - \kappa_2}{\kappa_1 + \kappa_2^*} \right| \left| \frac{\tau_0^2 + \kappa_1 \kappa_2}{\tau_0^2 - \kappa_1 \kappa_2^*} \right| \right), \tag{17}$$

in which the κ's are the complex soliton eigenvalues defined as $\kappa_j = a_j + i b_j$. Like most solitons, the dark-bright solitons are displaced most when the soliton eigenvalues nearly coincide. The main difference between this result and the equivalent result for arbitrarily polarized bright solitons (in focusing media) is that there is no equivalent of the ''polarization rotation'' that occurs for bright solitons. This is a consequence of the nonzero boundary conditions that remove one degree of freedom by comparison with the purely bright Manakov solitons.

Figure 7(a) shows the collision between two solitons of different directions and contrast. Longitudinal and transverse beating, invariably absent in collisions between scalar dark solitons, is clearly visible. Note that the amount of energy carried in the bound mode is an invariant of the equations,

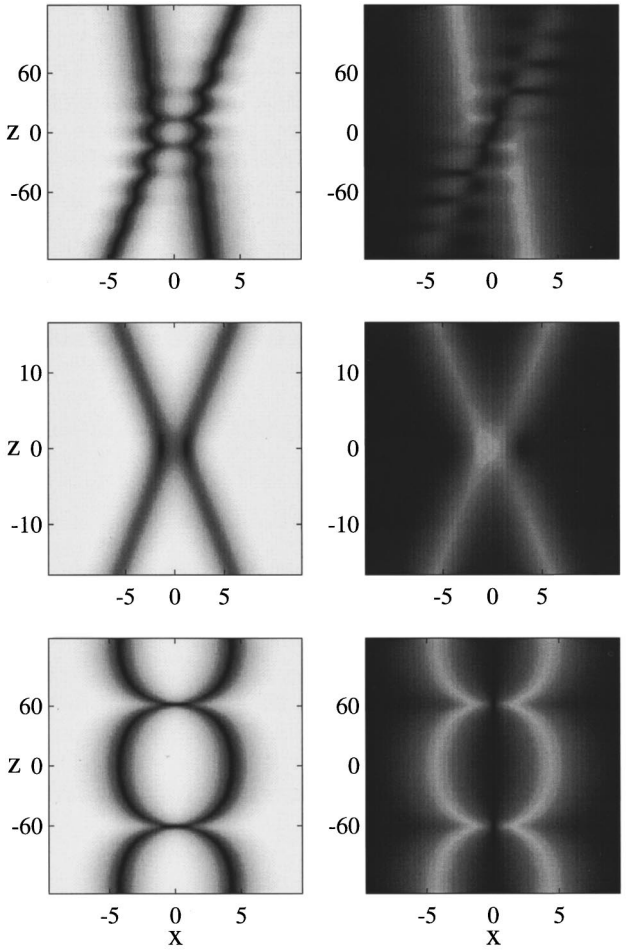

FIG. 7. Three examples of dark-bright soliton interactions. At left we show the amplitude of the dark-field component $|e_+|$, and at right $|e_-|$. In (a) we show a general collision in which $a_1 = 0.7$, $b_1 = -0.01$, $a_2 = 0.97$, and $b_2 = 0.03$, showing the beating phenomena. In (b) the solitons are mirror images of one another: $a_1 = a_2 = 0.7$ and $b_1 = -b_2 = 0.3$. In (c) we show a bound mode where the two solitons are coincident and almost equal in contrast, giving rise to very strong beating effects: $a_1 = 0.7$, $a_2 = 0.77$, and $b_1 = b_2 = 0$.

and therefore there is no change of the polarization state. For symmetric collisions such as in Fig. 7(b) there is no beating, since all components share the same propagation constant.

Unlike the focusing solitons of the Manakov system, the initial position of dark-bright solitons does not play a significant role. Consequently the general N-soliton solution is a straightforward generalization of the two soliton interaction and can be found using the Hirota method and is presented in Sec. 2 of the Appendix, Eq. (A18).

Asymptotics reveal the total position shift suffered by a soliton experiencing many collisions to be simply the sum of the shifts that it would suffer if each collision occurred separately. The interactions therefore commute, like the collisions of scalar solitons, and unlike vector bright soliton interactions.

IV. BOUND MODES AND STATIONARY STATES

Since these solitons possess both bright and dark components, one may expect them to exhibit a mixture of effects

normally associated with bright and dark solitons. In Fig. 7(a), one observes beating in the interaction between dark-bright solitons. We are accustomed to observing beating only in the interaction of bright solitons. Another phenomenon usually restricted to bright solitons is the existence of bound modes, or breather states. These solutions are special cases of N solitons in which each soliton travels in the same direction. The superposition of nonlinear modes results in a beating effect so that breathers of two solitons are periodic in z, as shown in Fig. 7(c). Higher-order breather states are quasiperiodic if the soliton amplitudes are not commensurate. Figure 8 shows an example of a three-soliton breather of noncommensurate eigenvalues that is consequently quasiperiodic.

Breather states are not strictly stable, since there is no binding energy between the constituent solitons. This is a property of all breather-type solutions in the integrable scalar NLS equation, and can be illustrated by considering the evolution of a minutely perturbed breather state. If the perturbation is asymmetric, then the velocities of the superposed solitons are no longer exactly equal, and therefore the solitons are no longer traveling perfectly in parallel. After enough distance the solitons will inevitably go their separate ways.

The general expression for the bound state between two dark-bright solitons can be found by rewriting Eq. (A17), with the imaginary parts of the soliton eigenvalues κ_1 and κ_2 equal (in other words, by making equal the propagation directions b_1 and b_2). In general, the bound states are asymmetric, since there are no solutions with equal eigenvalues, and the solitons are not coincident. If, however, the solitons are coincident, then the bound modes are symmetric in the dark component but antisymmetric in the bright part. All these properties are shared with bright soliton breathers of the Manakov model.

Bright Manakov solitons exhibit a special type of bound state that is completely stationary—i.e., there is no change in the total beam intensity along the direction of travel [23,24]. These stationary states exist when the two solitons are given orthogonal polarizations. Happily, it is also possible to suppress the beating between dark-bright solitons by making one of the solitons completely dark. The resultant family is completely analogous to the bright case, except that there is an additional degree of freedom: the ''greyness,'' or direction of travel relative to the background wave. One arrives at the formula for this by setting $a_1^2+b_1^2=\tau^2$, and setting the soliton directions b_1 and b_2 equal. Note that, for simplicity, we have also set $c=0$ and $\tau=1$. We can then write, for the dark component,

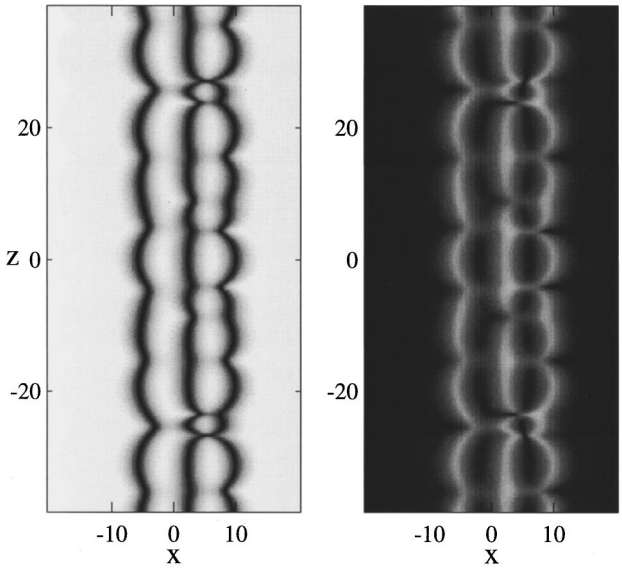

FIG. 8. A quasiperiodic interaction of three coincident dark-bright solitons, each one with the same position and direction, but each with different contrast, defined by $a_j=0.6$, 0.4, and 0.2.

$$e_+ = e^{-iz+i(\phi_1+\phi_2)}\ \frac{\cosh(\xi_1+i\phi_1+\xi_2+i\phi_2)-\Omega\cosh(\xi_1+i\phi_1-\xi_2-i\phi_2)}{\cosh(\xi_1+\xi_2)+\Omega\cosh(\xi_1-\xi_2)}, \tag{18}$$

and, for the bright component,

$$e_- = \frac{2(a_1+a_2)}{\sqrt{1+b^2/a_2^2}}e^{ibx+(i/2)(a_2^2-b^2)z} \times \frac{\sinh\xi_1}{\cosh(\xi_1+\xi_2)+\Omega\ \cosh(\xi_1-\xi_2)}, \tag{19}$$

where $\xi_j=a_j(x-\Delta x_j-bz)$ for $j=1$ and 2, $\Omega=(a_1+a_2)/(a_1-a_2)$, and $\phi_j=\arctan(b/a_j)$ gives a measure of the greyness of each soliton.

If the solitons almost coincide, then, as shown in Fig. 9(a), they form a closely knit bound state, while if the soliton positions are very different then each one propagates in isolation, and takes more or less the same profile that they would if the other were not there—which means that one of the solitons will be without a bright component altogether. This situation is shown in Fig. 9(b). If the positions exactly coincide then the solution is symmetric, and, for $a_2 \ll a_1$, the solitons are indistinguishable, as shown in Fig. 9(c). Conversely, as $a_2 \to a_1$, the solution evolves to two individual and identical dark-bright solitons with bright components out of phase with each other [Fig. 9(d)]. Quantitatively speaking, in the limit $a_2 \to a_1(1-\epsilon)$, the separation between the two solitons is $(1/a_1)\ln(2/\epsilon)$, and the amplitude of each of the bright components is $\sqrt{2\epsilon}\cos\phi$, showing that, for well separated solitons, the solitons are almost dark. It is not possible to form higher-order stationary states since only one of the parallel solitons can be totally dark (multisoliton solutions exist only for nondegenerate eigenvalues), and the remaining dark-bright solitons must beat against each other.

The stationary states are also important, purely on account of their static nature. The remainder of the multisoliton fam-

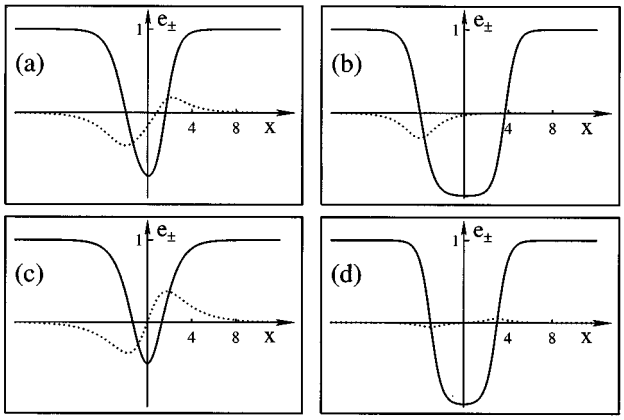

FIG. 9. The profiles of some stationary bound states of Manakov dark-bright solitons. In (a) and (b) we show stationary states formed from solitons that are parallel rather than coincident, resulting in bound states are asymmetric. In (c) and (d) the solitons are coincident and the states are symmetric. In (d) the solitons eigenvalues almost coincide and we observe the formation of two individual, almost completely dark, solitons, as described in the text. The parameters, from Eq. (19), are, for each image, $b=0$, $a_1=1$, and $\Delta x_1=-\Delta x_2$; specifically, in (a) $a_2=0.6$, $\Delta x=0.8$; (b) $a_2=0.8$, $\Delta x=2.6$; (c) $a_2=0.55$, $\Delta x=0.0$; and (d) $a_2=0.99$, $\Delta x=0.0$;

ily describes highly dynamic solutions such as perfectly elastic collisions or radiationless breather states: striking phenomena that are unfortunately confined to integrable models. Conversely, the lack of dynamics exhibited by the stationary states means that one would expect them to generalize and be found in nonintegrable systems.

V. DARK SOLITARY WAVES AND NONLINEAR ANISOTROPY

A more general model for an isotropic medium generalizes the nonlinear coupling to include a nonlinear anisotropy. We characterize this anisotropy with the parameter σ, and write the propagation equations in the form

$$i\frac{\partial e_{\pm}}{\partial z}+\frac{1}{2}\frac{\partial^2 e_{\pm}}{\partial x^2}-(|e_{\pm}|^2+\sigma|e_{\mp}|^2)e_{\pm}=0. \qquad (20)$$

Note that we have broken the symmetry possessed by the Manakov model, and the polarization components can no longer be chosen arbitrarily; $e_{\pm}$ represents the field strength in counter-rotating circular polarizations. More precisely, $e_{\pm}=(e_x\pm ie_y)/\sqrt{2}$, if e_x and e_y represent the decomposition of the field along the x and y axes. Physically the effect of σ is that each component now suffers a different refractive index change. The classical values of σ are 1, $\frac{2}{3}$, and 2, although numerous values have been suggested by a large number of theoretical and experimental studies. For $\sigma\neq 1$ this equation fails the Painlevé integrability test [25], and therefore does not support the propagation of true mathematical solitons. As a consequence, the solitary waves that one finds for $\sigma\neq 1$ will change and radiate energy in interaction with other solitary waves.

This section will summarize and describe the results of previous studies of the dark solitary waves of Eq. (20). These investigations have located a variety of dark-bright [26], dark-dark [8] and domain-wall-type solutions [27]. Being nonintegrable, Eq. (20) is not amenable to analytic methods such as that of Hirota.

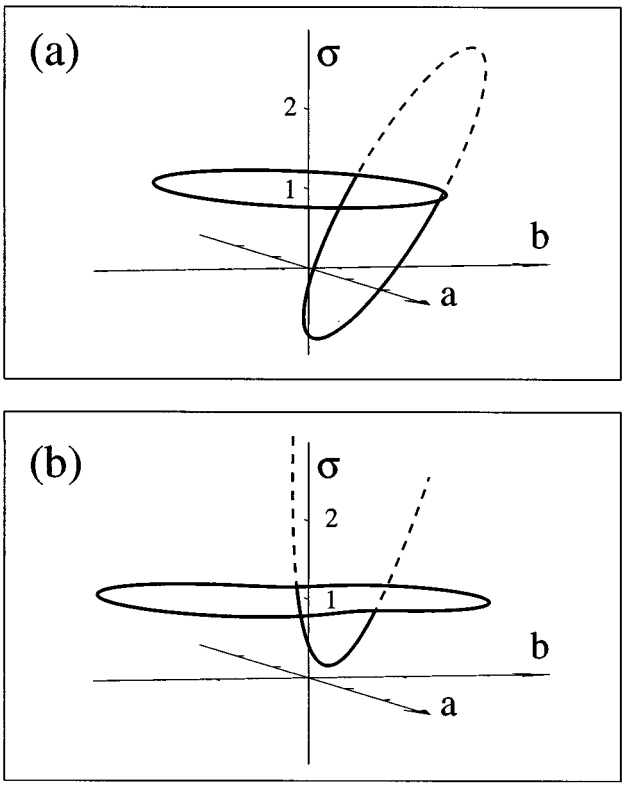

FIG. 10. The relationship between dark-dark Manakov solitons and the dark-dark solitary waves in systems exhibiting nonlinear anisotropy. We show the existence domains in (a,b) space, and as a function of the material parameter σ. The dashed curves indicate modulational instability of the solitary waves' backgrounds for $\sigma>1$. In (a) the backgrounds are quite closely aligned: $\tau_+=1$, $\tau_+=\sqrt{2}$, and $c_+=-c_-=0.5$, while in (b) they are as for Fig. 1(a): $c_+=-c_-=1.3$. Note that it is not yet clear whether there exists a wider class of solutions for $\sigma\neq 1$.

First, we discuss the dark-dark solitary waves. Analytical solutions have been found using an ansatz method [8]. These solutions are both an extension and a restriction of those solutions we presented in Eq. (10). They are more general, since they extend these solutions into the domain of nonintegrable models but more restricted since they impose an additional constraint

$$\tau_+^2\cos^2\phi_+=\tau_-^2\cos^2\phi_-. \qquad (21)$$

Figure 10 shows the relationship between these two solution families for two different background fields. In fact, the background plane waves of these structures become unstable for $\sigma>1$ due to the effect of polarization modulational instability [28,27]. We indicate this in the figure by rendering the solitary waves on the unstable backgrounds with a dashed line. General questions of stability of the dark-dark solitons are not dealt with in this work, however.

For these algebraically expressed dark-dark solitary waves, both components of the field suffer the same refractive index change

$$|e_+|^2+\sigma|e_-|^2=\sigma|e_+|^2+|e_-|^2. \quad (22)$$

For the Manakov model, i.e., for $\sigma=1$, this is trivially satisfied, but with a nonlinear anisotropy this represents a strong restriction. One could try to relax this condition by using analytical-numerical methods to find a more general class of solitary waves. We write the field in the form

$$e_\pm(x,z)=f_\pm(x)e^{i\phi_\pm(x)}\ e^{i\beta_\pm z}, \quad (23)$$

in which $f_\pm$ and $\phi_\pm$ are real functions. Substitution of this into Eq. (20) leads to real ordinary differential equations that can easily be treated numerically as a one-dimensional boundary value problem. This study has not yet been carried out, and it is not apparent to the authors whether or not the solution set of dark-dark solitary waves can be extended.

Much more is known and can be stated about the dark-bright solitary waves. The reason for this is that in linearizing about a scalar dark soliton of e_+, one can find bifurcation points at which the field e_- is the linear mode localized by the refractive index change caused by e_+. The existence of a simple bound mode is guaranteed for any positive value of the parameter σ. By proposing the stationary ansatz

$$e_+(x,z)=f_+(x)e^{i\phi(x)}e^{i\beta_+ z}, \quad e_-(x,z)=f_-(x)e^{i\beta_- z}, \quad (24)$$

then solving the resultant ordinary differential equations numerically, one can find broad families of dark-bright solitary waves that are not susceptible to polarization modulational instability since the background is a pure circular polarization state. This general dark-bright analysis awaits completion, although Ref. [26] used this approach on coupled nonlinear Schrödinger equations with opposite dispersions. Other works considered primarily the black-bright (i.e., $\phi=0$) solitary waves (24) [9]. For this case one finds, by analyzing the case of infinitesimal power in the component e_-, that there are bifurcation points on the line $\beta_-(2\beta_-+1)=\sigma$. Consequently one expects dark-bright solitary waves above this line. In addition, consideration of the mechanical analog of the differential equation system [9] allows us to foresee that the contrast will drop to zero on the line $\beta_-=\sigma$, bounding the domain from above. A further constraint is that β_- must remain smaller than β_+, since the eigenvalue of the fundamental mode (e_-) is always smaller than that of the first mode (e_+). It has been shown that in this limit $\beta_-\to\beta_+$, the solitary wave evolves into a state of two infinitely separated domain walls [9]. The domain of existence defined by these constraints is shown in Fig. 11.

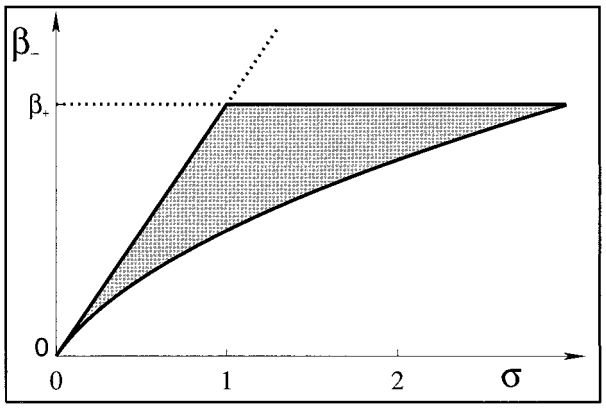

FIG. 11. Domain of existence of the black-bright ($\phi=0$) solitary waves in nonintegrable media. The lower bound on the domain is defined by the bifurcation point, at which the energy in the bound component is zero, while the upper bound either represents the greying out of the soliton (on the line $\beta=\sigma$), or the formation of two infinitely separated domain walls (where $\beta_-=\beta_+$).

VI. CONCLUSIONS

This paper explored the properties of dark-type Manakov solitons of nonuniform polarization. We found that they can be divided into two categories, that we label simply dark-dark and dark-bright solitons.

The dark-dark solitons represent an interesting vector generalization of the scalar dark soliton. The interplay between the two overlapping background fields affects the soliton's profile and existence in a complex manner. The dark-bright solitons are a more obvious generalization of scalar solitons. The bright component has the effect of reducing the soliton's contrast, but also of adding a degree of freedom, paving the way for surprising phenomena. Unlike traditional dark solitons, these solitons can attract one other and form bound modes, of which, exactly paralleling bright solitons, there is a family of stationary states.

Interlaced with the analytic results, we also discussed the possible consequences of our findings for more general nonintegrable models. Also incorporating the findings of previous studies, our work suggests that, as far as much of the phenomena presented here is concerned, the integrable system is a representative example of a wider class of models. Of particular interest is the expectation that dark-bright solitons would exhibit attractive and repulsive interactions, and form bound states in a variety of media.

APPENDIX: SOLUTION OF THE HIROTA EQUATIONS FOR DARK-BRIGHT SOLITONS

1. Single dark-bright solitons

Substitution of the quadratic ansatz Eq. (13) into the Hirota equations, Eq. (8), and equating coefficients of powers of λ, leads to the following series of equations:

$$\lambda^0: \quad B_1(g_0\cdot 1)=0, \quad B_2(1\cdot 1)=-|g_0|^2, \quad (A1)$$

$$\lambda^1: \quad B_1(h_1\cdot 1)=0, \quad (A2)$$

$$\lambda^2: \quad B_1(g_0g_2\cdot 1+g_0\cdot f_2)=0, \quad B_2(f_2\cdot 1+1\cdot f_2)=-|g_0|^2(g_2^*+g_2), \quad (A3)$$

$$\lambda^3: \quad B_1(h_1\cdot f_2)=0, \quad (A4)$$

$$\lambda^4: \quad B_1(g_0g_2\cdot f_2)=0, \quad B_2(f_2\cdot f_2)=-|g_0g_2|^2. \quad (A5)$$

We resolve this by starting at the lowest orders. At the zeroth order we find the solution for g_0 to be

$$g_0=\tau e^{icx+i[(1/2)c^2+\chi]z}, \quad (A6)$$

where $\tau^2=\chi$. Proceeding to the first order, we follow the standard path in the Hirota method by choosing a single exponential for h_1 of the form

$$h_1=e^{\eta}, \tag{A7}$$

where $\eta=\kappa x+i(\frac{1}{2}\kappa^2-\tau^2)z$ and $\kappa=a+bi$ is the complex eigenvalue. Note that, owing to the translational symmetry of the propagation equations, f_1 is defined only up to a multiplicative constant. At the second order,

$$f_2=\mu e^{\eta+\eta^*}, \tag{A8}$$

$$g_2=-(\rho/\rho^*)\mu e^{\eta+\eta^*}, \tag{A9}$$

where $\rho=a+i(b-c)$ and the coefficient μ takes the form

$$\mu=\left[(\kappa+\kappa^*)^2\left(\frac{\tau^2}{|\rho|^2}-1\right)\right]^{-1}. \tag{A10}$$

This defines the solution; calculations at higher orders reveal that Eqs. (A5) are satisfied to the fourth power of λ. A dark-bright soliton, then, is of the form

$$e_+=\tau\frac{1-\dfrac{\rho}{\rho^*}\mu e^{\eta+\eta^*}}{1+\mu e^{\eta+\eta^*}}e^{icx+i[(1/2)c^2+\tau^2]z}, \tag{A11}$$

$$e_-=\frac{e^{\eta}}{1+\mu e^{\eta+\eta^*}}. \tag{A12}$$

This solution can also be written in the more convenient form presented in the main text as Eq. (15).

2. Dark-bright multisoliton solutions

The calculation of this state is a tedious but straightforward algebraic exercise. We use the obvious quartic ansatz

$$g=g_0(1+\lambda^2 g_2+\lambda^4 g_4),\quad h=\lambda h_1+\lambda^3 h_3,\qquad f=1+\lambda^2 f_2+\lambda^4 g_4, \tag{A13}$$

and substitute this into the Hirota equations of Eq. (8), to derive the nine relations analogous to Eqs. (A5).

The solution to these equations is again found by beginning with the zeroth order. We choose exactly the same form again for g_0, since the background is not changed. At the first order, we choose

$$h_1=e^{\eta_1}+e^{\eta_2}, \tag{A14}$$

in which each term describes one soliton. Calculations then lead inexorably to the solution

$$e_+=\tau\frac{1-\displaystyle\sum_{j,k=1}^{2}\frac{\rho_j}{\rho_k^*}\mu_{jk}e^{\eta_j+\eta_k^*}+\frac{\rho_1\rho_2}{\rho_1^*\rho_2^*}f_4^0 e^{\eta_1+\eta_1^*+\eta_2+\eta_2^*}}{1+\displaystyle\sum_{j,k=1}^{2}\mu_{jk}e^{\eta_j+\eta_k^*}+f_4^0 e^{\eta_1+\eta_1^*+\eta_2+\eta_2^*}}e^{ip}, \tag{A15}$$

$$e_-=\frac{\displaystyle\sum_{j=1}^{2}e^{\eta_j}+\sum_{j=1}^{2}\nu_{jk}\mu_{1j}\mu_{2j}e^{\eta_1+\eta_1^*+\eta_j}}{1+\displaystyle\sum_{j,k=1}^{2}\mu_{jk}e^{\eta_j+\eta_k^*}+f_4^0 e^{\eta_1+\eta_1^*+\eta_2+\eta_2^*}}, \tag{A16}$$

where

$$\mu_{jk}=\left[(\kappa_j+\kappa_k^*)^2\left(\frac{|\tau_0|^2}{\rho_j\rho_k^*}-1\right)\right]^{-1},\qquad \nu_{jk}=(\kappa_j-\kappa_k)\left(\frac{|\tau_0|^2}{\rho_j\rho_k}+1\right),\qquad f_2^0=\mu_{11}\mu_{22}|\nu_{12}\mu_{12}|^2. \tag{A17}$$

Sadly there is no simple way to write this expression down; please see the discussion in the text on the characterization and visualization of this expression.

It is also possible to extend this expression so as to describe N-soliton solutions. The ansatz that one chooses is the obvious generalization of Eq. (A13), which leads to a series with three equations at each of the $2N+1$ orders of λ. The following prescription is the outcome of this procedure; substitution of it into the Hirota equations confirms that it describes the dark-bright N-soliton.

$$f=\sum M_1(a)\exp\left(\sum_{j=1}^{2N}a_j\eta_j+\sum_{1\leqslant j<k}^{2N}a_j a_k A_{j,k}\right),$$

$$g=\tau_0 e^{ip}\left[\sum M_2(a)\exp\left(\sum_{j=1}^{2N}a_j(\eta_j+\zeta_j)+\sum_{1\leqslant j<k}^{2N}a_j a_k A_{j,k}\right)\right], \tag{A18}$$

$$h=\sum M_1(a)\exp\left(\sum_{j=1}^{2N}a_j\eta_j+\sum_{1\leqslant j<k}^{2N}a_j a_k A_{j,k}\right),$$

where the first sum is over all possible permutations of the vector $a=(a_1,a_2,\ldots,a_{2N})$, in which each a_j can be either 0 or 1. The previous definitions for the two-soliton solution are extended as

$$\eta_{j+N}=\eta_j^*,\quad \zeta_{j+N}=1/\rho_j^*,\quad e^{A_{j,k+N}}=\mu jk,\qquad e^{A_{j+N,k}}=\mu_{jk}^*,\quad e^{A_{j,k}}=\nu_{jk},\quad e^{A_{j+N,k+N}}=\nu_{jk}^* \tag{A19}$$

and

$$M_1=\begin{cases}1 & \text{if } \displaystyle\sum_{j=1}^{N}a_j=\sum_{j=N+1}^{2N}a_j\\ 0 & \text{otherwise,}\end{cases} \tag{A20}$$

$$M_2=\begin{cases}1 & \text{if } \displaystyle\sum_{j=1}^{N}a_j=\sum_{j=N+1}^{2N}a_j+1\\ 0 & \text{otherwise.}\end{cases}$$

[1] A. Hasegawa, *Solitons in Optical Fibres* (Springer-Verlag, New York, 1989).
[2] R. De la Fuente, A. Barthelemy, and C. Froehly, Opt. Lett. **16**, 793 (1991).
[3] M. Shalaby and A. Barthelemy, Opt. Lett. **16**, 1472 (1991).
[4] J. S. Aitchison *et al.*, Opt. Lett. **16**, 15 (1991).
[5] Y. S. Kivshar, IEEE J. Quantum Electron. **29**, 250 (1993).
[6] P. Emplit *et al.*, Opt. Commun. **62**, 347 (1987).
[7] B. Luther-Davies and X. Yang, Opt. Lett. **17**, 496 (1992).
[8] Y. S. Kivshar and S. K. Turitsyn, Opt. Lett. **18**, 337 (1993).
[9] M. Haelterman and A. P. Sheppard, Phys. Rev. E **49**, 4512 (1994).
[10] R. Radhakrishnan and M. Lakshmanan, J. Phys. A **28**, 2683 (1995).
[11] R. W. Boyd, *Nonlinear Optics* (Academic, New York, 1992).
[12] D. H. Close *et al.*, IEEE J. Quantum Electron. **2**, 553 (1966).
[13] S. G. Evangelides, L. F. Mollenauer, and J. P. Gordon, IEEE J. Lightwave. Technol. **10**, 28 (1992).
[14] P. K. A. Wai and C. R. Menyuk, IEEE J. Lightwave. Technol. **14**, 148 (1996).
[15] J. U. Kang, G. I. Stegeman, J. S. Aitchison, and N. N. Akhmediev, Phys. Rev. Lett. **76**, 3699 (1996).
[16] J. U. Kang, G. I. Stegeman, and J. S. Aitchison, Opt. Lett. **21**, 189 (1996).
[17] S. V. Manakov, Zh. Eksp. Teor. Fiz. **65**, 505 (1973) [Sov. Phys. JETP **38**, 248 (1974)].
[18] A. C. Newell and J. V. Moloney, *Nonlinear Optics* (Addison-Wesley, Redwood City, CA, 1992).
[19] A. Villeneuve, J. U. Kang, and G. I. Stegeman, Appl. Phys. Lett. **67**, 760 (1995).
[20] V. E. Zakharov and A. B. Shabat, Zh. Eksp. Teor. Fiz. **61**, 118 (1971) [Sov. Phys. JETP **34**, 62 (1972)].
[21] V. E. Zakharov and A. B. Shabat, Zh. Éksp. Teor. Fiz. **64**, 1627 (1973) [Sov. Phys. JETP **37**, 823 (1973)].
[22] R. Hirota, Phys. Rev. Lett. **27**, 1192 (1971).
[23] D. N. Christodoulides and R. I. Joseph, Opt. Lett. **13**, 53 (1988).
[24] M. V. Tratnik and J. E. Sipe, Phys. Rev. A **38**, 2011 (1988).
[25] R. Sahadevan, K. M. Tamizhmani, and M. Lakshmanan, J. Phys. A **19**, 1783 (1986).
[26] A. V. Buryak, Y. S. Kivshar, and D. F. Parker, Phys. Lett. A **215**, 57 (1996).
[27] M. Haelterman and A. P. Sheppard, Phys. Rev. E **49**, 3376 (1994).
[28] A. L. Berkhoer and V. E. Zakharov, Zh. Eksp. Teor. Fiz. **58**, 903 (1970) [Sov. Phys. JETP **31**, 486 (1970)].